Molecular Biology of the Cell
Vol. 21, 2987–2995, September 1, 2010

Selective Association of Peroxiredoxin 1 with Genomic DNA and *COX*-2 Upstream Promoter Elements in Estrogen Receptor Negative Breast Cancer Cells

Xuemei Wang, Shihua He, Jian-Min Sun, Geneviève P. Delcuve, and James R. Davie

Manitoba Institute of Cell Biology, University of Manitoba, Winnipeg, Manitoba R3E 0V9, Canada

Submitted February 24, 2010; Accepted June 28, 2010
Monitoring Editor: Kunxin Luo

In a search for proteins differentially cross-linked to DNA by cisplatin or formaldehyde in normal breast epithelial and breast cancer cell lines, we identified peroxiredoxin 1 (PRDX1) as a protein preferentially cross-linked to DNA in estrogen receptor negative (ER−) MDA-MB-231 but not in estrogen receptor positive (ER+) MCF7 breast cancer cells. Indirect immunofluorescence microscopic analyses showed that PRDX1 was located in the cytoplasm and nucleus of normal and breast cancer cells, with nuclear PRDX1 associated with promyelocytic leukemia protein bodies. We demonstrated that PRDX1 association with the transcription factor nuclear factor-κB (NF-κB) in MDA-MB-231 but not in MCF7 cells contributed to PRDX1-selective recruitment to MDA-MB-231 genomic DNA. Furthermore, PRDX1 was associated with the *cyclooxygenase* (*COX*)-2 upstream promoter region at sites occupied by NF-κB in ER− but not in ER+ breast cancer cells. PRDX1 knockdown attenuated *COX*-2 expression by reducing NF-κB occupancy at its upstream promoter element in MDA-MB-231 but not in MCF7 cells. A phosphorylated form of PRDX1 was only present in ER− breast cancer cells. Because PRDX1 phosphorylation is known to inhibit its peroxidase activity and to promote PRDX1 oligomerization, we propose that PRDX1 acts as a chaperone to enhance the transactivation potential of NF-κB in ER− breast cancer cells.

INTRODUCTION

Breast cancer is the most commonly diagnosed cancer in women in North America and Europe, second only to lung cancer in mortality rate. It has been hypothesized that breast tumorigenesis is a result of cumulative changes that lead to the transformation of normal epithelium to abnormal cellular modifications resulting in hyperplasia, atypical hyperplasia, ductal carcinoma in situ, and invasive carcinoma. Finally, all these changes culminate into metastasis (Allred *et al*., 1993). Although breast cancer is characterized by heterogeneity and various prognostic outcomes, it has been shown that the wide diversity of genomic and transcriptional abnormalities present in primary breast tumors is well represented in human breast cancer cell lines (Neve *et al*., 2006; Zhu *et al*., 2006; Vargo-Gogola and Rosen, 2007).

Transcription factors, cofactors, and architectural proteins contribute to gene expression programming in normal and disease states. Changes in the spectrum of these proteins directly or indirectly bound to DNA impact gene programming of normal and cancer cell types. A research tool to identify the proteins associated with genomic DNA is in situ cross-linking by cisplatin [*cis*-platinum(II)diamminedichloride; *cis*-DDP] (Ferraro *et al*., 1992; Spencer and Davie, 2002a). Cisplatin directly cross-links proteins to DNA, but not to other proteins, and many DNA cross-linked proteins are nuclear matrix proteins. We have shown that cisplatin cross-links nuclear matrix-associated transcription factors and cofactors (estrogen receptor, Hsp27 ERE-TATA binding protein/scaffold attachment factor B, heterogeneous nuclear ribonucleoprotein K [hnRNP K], histone deacetylases [HDACs 1 and 2 but not 3]) to DNA in the MCF7 human breast cancer cell line (Samuel *et al*., 1998; Davie *et al*., 1999; Sun *et al*., 2002, 2007). These transcription factors and cofactors are crucial to the organization and structure of chromatin and to the regulation of genes involved in the proliferation of breast cancer cells. Histones are poorly cross-linked to DNA by cisplatin. Nuclear proteins such as SRm160 and carboxypeptidase are not cross-linked to DNA with cisplatin (Samuel *et al*., 1998; Chichiarelli *et al*., 2002). Analyses of two-dimensional gel patterns of proteins cross-linked to DNA in situ with cisplatin led to the identification of proteins that were differentially bound to DNA in hormone-dependent and -independent human breast cell lines (Spencer *et al*., 2000) or in hormone-dependent cell lines representing different stages of malignant progression in breast cancer (Spencer *et al*., 2001). Thus, cisplatin is a useful cross-linking agent to identify transcription factors, cofactors, and other DNA-associated proteins involved in DNA organization and transcription of cancer cells.

In this study, we analyzed the proteins cross-linked to nuclear DNA by cisplatin in situ in a panel of human breast normal and cancer cell lines, including the nontumorigenic MCF10A1 cell line; the estrogen receptor positive (ER+), estrogen-dependent MCF7 and T-47D cancer cell lines; and the estrogen receptor negative (ER−), estrogen-inde-

This article was published online ahead of print in *MBoC in Press* (http://www.molbiolcell.org/cgi/doi/10.1091/mbc.E10–02–0160) on July 14, 2010.

Address correspondence to: James R. Davie (davie@cc.umanitoba.ca).

pendent MDA-MB-231, MDA-MB-468, and BT-20 cancer cell lines.

The research objective was to identify proteins differentially cross-linked to the DNA of these cell lines, to pinpoint aberrant molecular behaviors involved in the differential gene programming of estrogen-responsive or estrogen-nonresponsive breast tumors. We identified peroxiredoxin 1 (PRDX1) as a protein differentially cross-linked in ER− versus ER+ cell lines. In an attempt to identify the molecular mechanism that drives the selective recruitment of PRDX1 to the genomic DNA of ER− cell lines, we found that PRDX1 associates with nuclear factor-κB (NF-κB), and both proteins are bound together to the *cyclooxygenase* (*COX*)-*2* upstream promoter region in ER− but not ER+ breast cancer cells. Knocking down PRDX1 resulted in the attenuation of *COX-2* expression in ER− but not ER+ breast cancer cells. In the PRDX1 knockdown ER− cells, NF-κB occupancy of the *COX-2* upstream promoter element was reduced. We further present evidence suggesting that this interaction with NF-κB is independent of PRDX1 peroxidase activity.

MATERIALS AND METHODS

Cell Culture

The human breast cancer cell lines, ER+ (MCF7 and T-47D) and ER− (MDA-MB-231, MDA-MB-468, and BT-20) were grown as described previously (Samuel *et al*., 1997). Immortalized breast epithelial MCF10A1 cells were grown as described in Coutts *et al*. (1999). Normal human mammary epithelial cells (HMECs) were purchased from Lonza Walkersville (Walkersville, MD) and grown according to the manufacturer's instructions. For some studies, MCF7 and MDA-MB-231 cells were treated with 1 mM H_2O_2 for 30 min.

Isolation and Analysis of Proteins Cross-Linked to DNA

In situ cross-linking of proteins to DNA by cisplatin or formaldehyde, their subsequent isolation and resolution by two-dimensional (2D) electrophoresis were described previously (Spencer *et al*., 2000; Sun *et al*., 2002; Spencer and Davie, 2002a,b). Proteins samples on 2D gels were either silver stained, imaged using Molecular Imager Fx (Bio-Rad Laboratories, Hercules, CA), and analyzed with the PDQuest 2-D analysis software, version 7.3.1 (Bio-Rad Laboratories) (50 μg) or stained with CBB G250 (Sigma-Aldrich, St. Louis, MO) and in-gel digested for identification (500 μg), or transferred onto nitrocellulose membranes and immunochemically stained with anti-PRDX1 antibodies (20 μg) (Abcam, Cambridge, MA). In-gel digestion, nano-liquid chromatography, and tandem mass spectrometry were performed essentially as described previously (Meng and Wilkins, 2005), except that the gel pieces dehydrated in acetonitrile were reduced in 10 mM dithiothreitol and subsequently alkylated with 55 mM iodoacetamide. To identify peptides, the MSDB, version 20060831 database was searched using the Global Proteome Machine (http://www.thegpm.org) search engine.

Cellular Fractionation, Immunoblotting, and Immunoprecipitation

Total cell lysates and nuclear and cytosolic extracts were obtained as described previously (Sun *et al*., 2001). Immunoblot analysis and immunoprecipitation were performed as described previously (Sun *et al*., 2002). Polyclonal antibodies against human PRDX1 (Abcam), glyceraldehyde-3-phosphate dehydrogenase (GAPDH; Abcam), HDAC1 (Affinity BioReagents, Golden, CO), PRDX1-SO_3 (Abfrontier, Seoul, Korea), and NF-κB p65 (Millipore, Billerica, MA), and monoclonal antibodies against human β-actin (Sigma-Aldrich) or TATA binding protein (TBP; Abcam) were used.

Fluorescence Microscopy

Indirect immunofluorescence was performed as described previously (He *et al*., 2005). Antibodies against PRDX1 (Abcam) or SC35 (Abcam) and promyelocytic leukemia (PML) protein (Santa Cruz Biotechnology, Santa Cruz, CA) were used. The 100 z-stack images of each color channel were taken at 200-nm increments with corresponding filters (Chroma Technology, Bellows Falls, VT) and an Axio Imager Z1 microscope and AxioCam HR charge-coupled device camera (Carl Zeiss, Oberkochen, Germany). Constrained iterative deconvolution of all color channels was performed for each color channel with AxioVision 4.4 software (Carl Zeiss).

Chromatin Immunoprecipitation (ChIP)

ChIP and re-ChIP assays were done on MCF7 and MDA-MB-231 cells as described previously (Li and Davie, 2008). The ChIP and input DNA concentrations were determined with the Quant-iT Picogreen dsDNA kit (Invitrogen, Carlsbad, CA). Equal amounts (2 ng) of ChIP and input DNAs were quantitated by real-time polymerase chain reaction (PCR), by using the two following pairs of primers: pair 1, forward, 5′-GTCAGCCTTTCTTAACCTTAC-3′ and reverse, 5′-CAGTCTTTGCCCGAGCGCTTC-3′ to amplify a 238-base pair fragment including the -439 NF-κB binding site; and pair 2, forward, 5′-GCCCTCCCCCGGTATCCCATC-3′ and reverse, 5′-AAAAAATTGCGTAAGCCCGGT-3′ to amplify a 262-base pair fragment including the -214 NF-κB binding site, in the promoter region of the *COX-2* gene. The enrichment values (ChIP DNA vs. input DNA) were calculated as follows: fold enrichment = $R^{(Ct\ input-Ct\ ChIP)}$, where R is the rate of amplification.

Protein Phosphatase Digestion

Total cell lysates or DNA cross-linked protein fractions were incubated with or without calf intestinal alkaline phosphatase (CIP; GE Healthcare, Little Chalfont, Buckinghamshire, United Kingdom) at 37°C for 1 h, resolved on two-dimensional gels, and immunoblotted with anti-PRDX1 antibodies.

Generation and Maintenance of PRDX1 Stable Knockdown MDA-MB-231 and MCF7 Cells

Empty GIPZ lentiviral vector, GIPZ scramble vector, and the GIPZ Lentiviral microRNA-adapted short hairpin RNA (shRNA) clones for human PRDX1 (clone V2LHS_152610 (G1) and clone V2LHS_152606 (G2) (Thermo Scientific Open Biosystems, Huntsville, AL) were obtained from the Biomedical Functionality Resource at University of Manitoba. PRDX1 stable knockdown MDA-MB-231 and MCF7 cell lines were obtained as described previously (Drobic et al., 2010).

RNA Isolation and Real-Time Reverse Transcription (RT)–PCR Analysis

Total RNA was isolated using RNeasy Mini kit (QIAGEN, Valencia, CA) following the manufacturer's instructions. The isolated RNA was used to synthesize the first-strand cDNA with the Moloney murine leukemia virus reverse transcriptase kit and oligo$(dT)_{12-18}$ primer (Invitrogen). Real-time PCR analysis was performed on iCycler IQ5 (Bio-Rad Laboratories) by using SYBR Green for labeling. Primer sequences are as follows: 5′-AAGAAACTCAACTGCCAAGTG-3′ (forward) and 5′-CAGCCTTTAAGACCCCATAAT-3′ (reverse) for *PRDX1*; 5′-CTGATTCAAATGAGATTGTGG-3′ (forward) and 5′-CCCTCGCTTATGATCTGTCT-3′ (reverse) for *COX-2*; and 5′-CAAGGCTGTGGGCAAGGTCATCC-3′ (forward) and 5′-GAGGAGTGGGTGTCGCTGTTGAAGT-3′ (reverse) for human *GAPDH*. The relative levels of *PRDX1* and *COX-2* gene expression were normalized to *GAPDH* levels.

RESULTS

PRDX1 Is Cross-Linked to DNA by Cisplatin In Situ in ER− but Not ER+ Human Breast Cancer Cell Lines

To identify proteins differentially bound to genomic DNA in ER−, ER+, and pseudonormal breast cancer cell lines, we compared the two-dimensional-gel patterns of proteins cross-linked with cisplatin to genomic DNA. Proteins cross-linked to DNA in cells with cisplatin were captured on hydroxyapatite. Protein–DNA cross-links were reversed with thiourea, and the proteins were isolated and resolved by two-dimensional polyacrylamide gel electrophoresis (PAGE). Figure 1 shows a protein, BC13, that was present among the proteins associated with the nuclear DNA of MDA-MB-231, an ER−, hormone-independent breast cancer cell line with high metastatic potential, but absent from the proteins associated with the nuclear DNA of MCF7, an ER+, hormone-dependent breast cancer cell line and absent from the proteins associated with the nuclear DNA of the nontumorigenic MCF10A1 cell line. Using mass spectrometry (in-gel digestion, nano-liquid chromatography, and tandem mass spectrometry), the BC13 protein, with a molecular mass of 22 kDa and a p*I* of 8.3, was identified as PRDX1. To verify the identification of BC13 as PRDX1, an immunoblot analysis using anti-PRDX1 antibodies was performed on samples of proteins isolated by cross-linking to DNA with cisplatin in a panel of human breast cells (Figure 2A). HDAC1, which we have shown previously to be cross-linked to DNA by cisplatin or formaldehyde (Sun *et al*., 2007), also was detected by immunoblot, whereas the cyto-

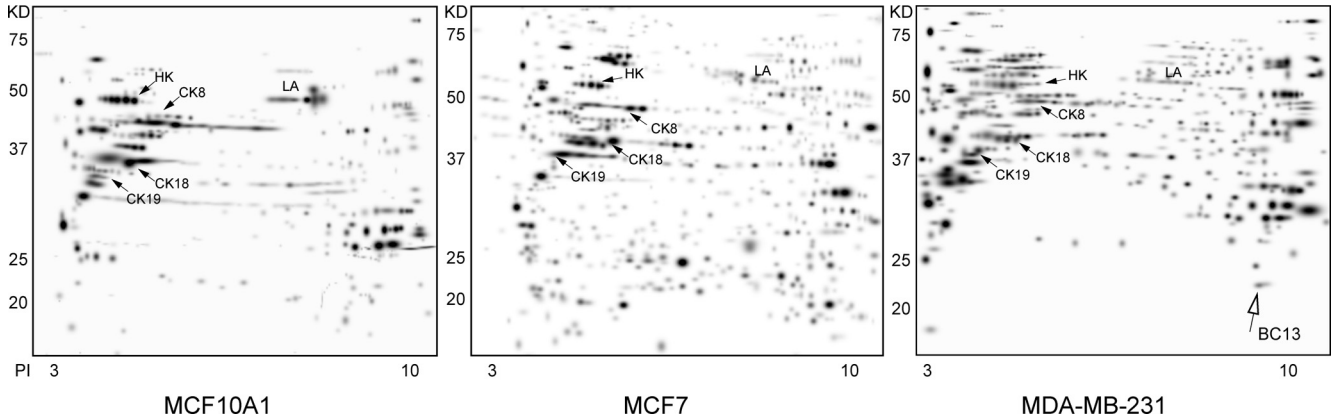

Figure 1. Proteins cross-linked to DNA by cisplatin in situ in MCF10A1, MCF7, and MDA-MB-231 human breast cell lines. DNA cross-linked proteins (50 μg) from cells treated with 1 mM cisplatin were electrophoretically resolved on two-dimensional gels. The gels were stained with silver. LA, HNRNPK, CK8, CK18, and CK19 point to the positions of lamin A; heterogeneous nuclear ribonucleoprotein K; and cytokeratins 8, 18, and 19, respectively. Data are representative of seven independent experiments.

plasmic protein GAPDH was not (Figure 2B). Figure 2A shows that PRDX1 was bound to DNA in ER− breast cancer MDA-MB-231 cells but not in normal HMEC cells obtained from reductive mammoplasty, pseudonormal MCF10A1 cells, or ER+ breast cancer MCF7 cells. PRDX1 also was differentially cross-linked in situ with formaldehyde to the DNA of MCF10A1, MCF7, and MDA-MB-231, with PRDX1 bound to the DNA of MDA-MB-231 but not MCF7 or MCF10A1 cells (Figure 2C). The lack of cisplatin cross-linking of PRDX1 to DNA also was observed with MCF7 cells cultured under estrogen-deplete conditions (data not shown).

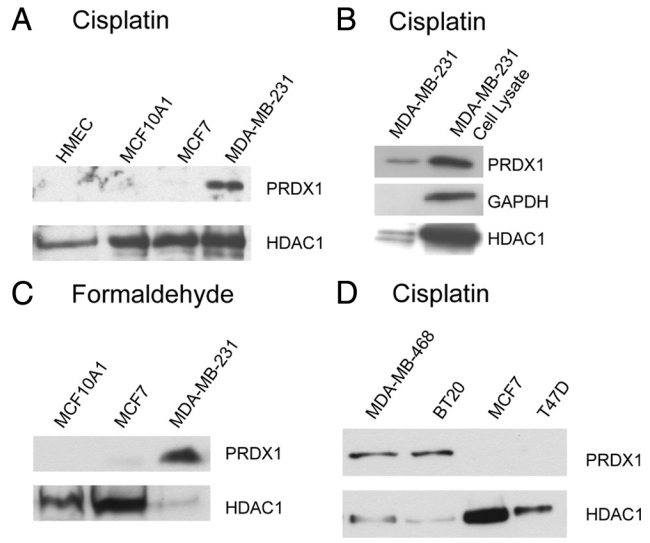

Figure 2. PRDX1 cross-linked to DNA by cisplatin in situ in MDA-MB-231 and other ER− human breast cell lines. DNA cross-linked proteins (20 μg) from cells treated with 1 mM cisplatin (A and D) or 1% formaldehyde (C) were resolved by SDS-10% PAGE and immunoblotted with anti-PRDX1 or anti-HDAC1 antibodies. (B) DNA cross-linked proteins (20 μg) from MDA-MB-231 cells treated with 1 mM cisplatin in the left lane, and proteins (20 μg) from MDA-MB-231 cell lysates. The blots were immunostained with anti-PRDX1, anti-GAPDH, or anti-HDAC1 antibodies. Data are representative of two and three independent experiments for formaldehyde and cisplatin cross-linking, respectively.

To establish the generality of our observations, we determined whether PRDX1 was differentially cross-linked with cisplatin in ER− and ER+ cells. Figure 2D shows that PRDX1 was cross-linked in situ by cisplatin to the DNA of MDA-MB-468 and BT20 cells, two other ER− cell lines, whereas PRDX1 was not cross-linked to the DNA of the ER+ T47D cell line.

PRDX1 Is Found in the Cytoplasm and Nucleus

It has been reported that PRDX1 was overexpressed in human breast cancer in comparison with normal tissues (Noh *et al.*, 2001). To compare the PRDX1 levels in our panel of cell lines, we did an immunoblot analysis on total cell extracts, using anti-PRDX1 antibodies. Figure 3A shows that the ER+ MCF7 and ER− MDA-MB-231 cancer cell lines had higher PRDX1 levels than the MCF10A1 pseudonormal cell line, which itself displayed higher PRDX1 levels than the HMEC normal cell line. Next, an immunoblot analysis with anti-PRDX1 antibodies was performed on nuclear extracts, using the TBP as a reference protein. Nuclear PRDX1 levels were

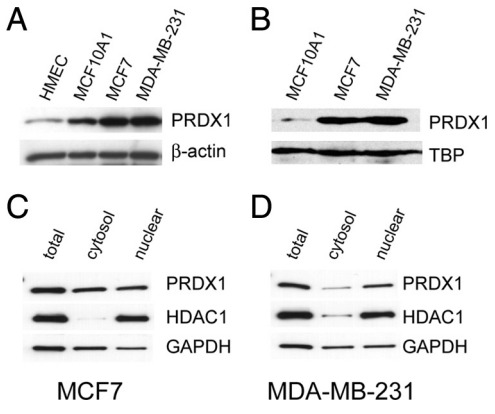

Figure 3. PRDX1 found in cytosol and nucleus of human breast normal and cancer cell lines. Proteins (20 μg) from total cell lysates (A), nuclear extracts (B), and total cell lysates and cellular fractions (C) were resolved by SDS-10 or 15% PAGE (with equal volumes of cytosol and nuclear samples loaded) and immunoblotted with anti-PRDX1, anti-β-actin, anti-TBP, anti-GAPDH, or anti-HDAC1 antibodies. Data are representative of three independent experiments.

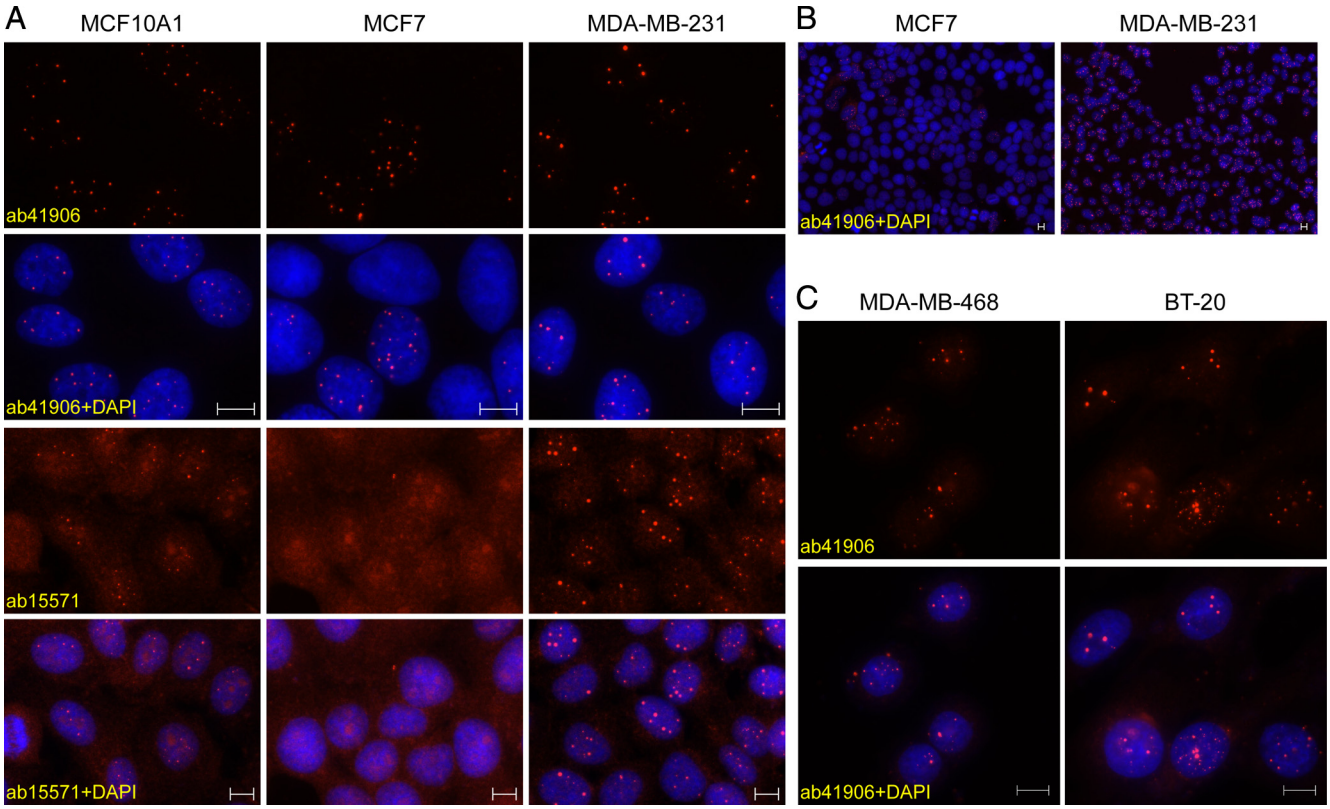

Figure 4. PRDX1 nuclear foci are more intense in MDA-MB-231 than in MCF7 cells. Human breast cells were subjected to indirect immunofluorescence labeling with anti-PRDX1 ab41906 or ab15571 antibodies, costained with 4,6-diamidino-2-phenylindole (DAPI), and digitally imaged. (A) PRDX1 distribution was visualized in MCF10A1, MCF7, and MDA-MB-231 cells, with indicated antibodies. (B) PRDX1 distribution in MCF7 and MDA-MB-231 cells was detected with anti-PRDX1 ab41906 antibody, and is shown at a lower amplification. (C) PRDX1 distribution in MDA-MB-468 and BT-20 cells was detected with anti-PRDX1 ab41906 antibody. Bar, 10 μm. Data are representative of three independent experiments.

greater in the ER+ MCF7 and ER− MDA-MB-231 cancer cell lines than in the MCF10A1 pseudonormal cell line (Figure 3B).

Previous studies reported that PRDX1 was primarily located in the cytosol (Wood *et al*., 2003). To assess the partitioning of PRDX1 between cytosol and nucleus, total cellular extracts from MCF7 and MDA-MB-231 were prepared and then fractionated into cytosol and nuclear extracts. All fractions were subjected to immunoblot analysis with anti-PRDX1 and anti-HDAC1 antibodies. HDAC1 was primarily found in the nuclear fractions as expected, whereas PRDX1 was present in both the cytosol and nucleus of MCF7 and MDA-MB-231 cells, with the cytosol levels being slightly lower than the nuclear levels (Figure 3C). However, the cytoplasmic GAPDH also was present in the nuclear fraction, demonstrating that nuclear fraction still had cytoplasmic proteins.

To further explore the cellular distribution of PRDX1, indirect immunofluorescence imaging was performed on cells grown and fixed on coverslips. In Figure 4A, PRDX1 detected with the anti-PRDX1 (ab41906) antibody appeared mostly as nuclear foci in MCF10A1, MCF7, and MDA-MB-231 cells, with the intensity of the foci being the greatest in MDA-MB-231 cells. On longer exposure, cytoplasmic PRDX1 also was observed. The specificity of the ab41906 antibody was demonstrated by the absence of immunofluorescent signal when the labeling was done in the presence of a peptide block (data not shown). When PRDX1 was visualized with another anti-PRDX1 antibody (ab15571), PRDX1 staining in the cytosol and nucleus was visible in MCF10A1, MCF7, and MDA-MB-231 cells, with the stained bodies seeming bigger and more diffuse in MCF7 cells (Figure 4A). Figure 4A also shows that, regardless of the anti-PRDX1 (ab41906 or ab15571) antibodies, PRDX1 nuclear foci were more intense in MDA-MB-231 than in MCF7 cells. Anti-PRDX1 (ab41906 or ab15571) antibodies, PRDX1 nuclear foci were more intense in MDA-MB-231 than in MCF7 cells. Figure 4B shows a large number of MCF7 and MDA-MB-231 cells in which PRDX1 was detected with the anti-PRDX1 (ab41906) antibody. Again, nuclear foci in MDA-MB-231 cells were more intense than in MCF7 cells. Moreover, every MDA-MB-231 cell displayed PRDX1 nuclear foci, whereas only a subset of MCF7 cells had them (Figure 4B). Indirect immunofluorescence imaging also was performed, using the anti-PRDX1 (ab41906) antibody on MDA-MB-468 and BT-20 cells (Figure 4C). For each of these ER− breast cancer cell lines, PRDX1 intense nuclear foci and cytosolic staining were apparent.

As shown in Figure 4, we observed variability in immunofluorescence imaging, particularly with MCF7 cells and less so for MDA-MB-231 cells. With different lots of the anti-PRDX1 antibody (ab15571, ab41906, and 07-609 [Millipore]; data not shown), we observed nucleolar staining in MCF7 cells (Figure 4A, ab15571), similar to that reported previously (Immenschuh *et al*., 2003). However, regardless of the anti-PRDX1 antibody used, we always observed bright staining foci in the nucleus of MDA-MB-231 cells and less intense staining nuclear foci in MCF10A1 cells.

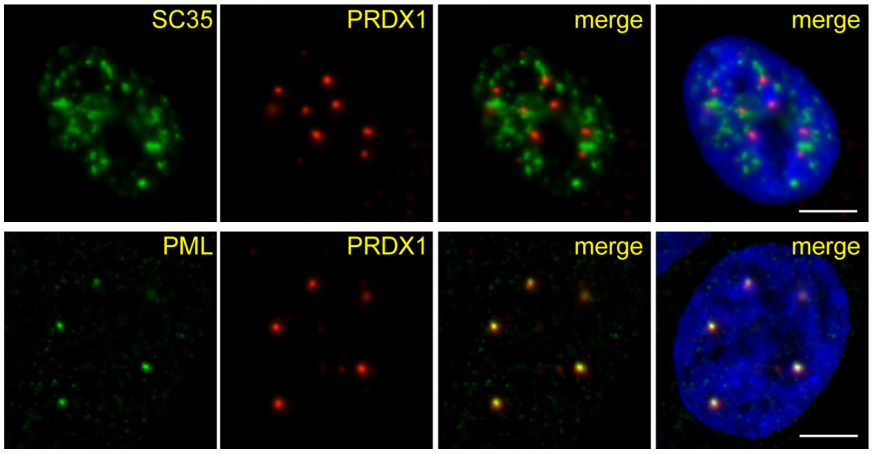

Figure 5. PRDX1 is colocalized with PML bodies in MDA-MB-231 cell line. Top, MDA-MB-231 cells, grown on coverslips, were fixed and double labeled with antibodies raised against SC35 and PRDX1. Bottom, MDA-MB-231 cells, grown on coverslips, were fixed and double labeled with antibodies raised against PML and PRDX1. DNA was stained with 4,6-diamidino-2-phenylindole (DAPI). SC35, PML, and PRDX1 distributions were visualized by fluorescence microscopy and image deconvolution as described in *Materials and Methods*. Single optical sections are shown. Yellow in the merged images signifies colocalization. Bar, 5 μm. Data are representative of three independent experiments.

To identify the nuclear body that PRDX1 was associated with, we first determined whether PRDX1 was localized with nuclear speckles, also called interchromatin granule clusters (IGCs). IGCs are dynamic structures enriched in pre-mRNA splicing factors and number 25–50 per cell (Spector, 2006). MDA-MB-231 cells grown and fixed on coverslips were double-labeled with anti-PRDX1 and anti-SC35 antibodies and visualized by fluorescence microscopy and image deconvolution (Figure 5). There was no colocalization of the PRDX1 and SC35 signals. However, the PRDX1-associated bodies were localized on the boundaries of the IGCs, which is a common feature of the PML bodies (Ishov *et al.*, 1997; Batty *et al.*, 2009). To determine whether nuclear PRDX1 was associated with PML bodies, we compared their spatial distributions in MDA-MB-231 cells by using indirect immunofluorescence microscopic analyses. Figure 5 shows that all PRDX1-associated nuclear bodies colocalized with PML bodies.

PRDX1 and NF-κB Are Bound Together to the COX-2 Upstream Promoter Region in MDA-MB-231 Cells

Because PRDX1 is not a DNA-binding protein, we considered a likely mechanism of PRDX1 recruitment to genomic DNA was by association with a transcription factor. It has been demonstrated that PRDX1 increased the transactivation potential of NF-κB in HeLa cells (Hansen *et al.*, 2007). Thus, we investigated whether PRDX1 was associated with NF-κB and whether the interaction between these two proteins was observed in ER− but not in ER+ breast cancer cells. MCF7 and MDA-MB-231 cell lysates were incubated with antibodies raised against PRDX1 or the p65 subunit of NF-κB, and the total cell lysates and immunoprecipitated fractions were analyzed by immunoblot. With MCF7 cell extracts, p65 was not coimmunoprecipitated with PRDX1 and vice versa, PRDX1 did not coimmunoprecipitate with p65 (Figure 6A). However, in MDA-MB-231 cell extracts, PRDX1 and p65 were coimmunoprecipitated with either anti-PRDX1 or anti-p65 antibodies (Figure 6B). Thus, PRDX1 and NF-κB are associated with each other in ER− MDA-MB-231 but not in ER+ MCF7.

Next, we investigated whether PRDX1 was associated with NF-κB in an upstream promoter region containing a NF-κB binding site. We selected the *COX-2* gene for study because NF-κB has a pivotal role in the expression regulation of *COX-2*, a gene that has a role in breast cancer (Singh-Ranger *et al.*, 2008). First, we determined the expression levels of *COX-2* in MCF7 and MDA-MB-231cells. Figure 7A shows that, relative to *GAPDH* levels, *COX-2* levels were greater in MDA-MB-231 than in MCF7 cells. To determine whether PRDX1 was associated with the *COX-2* upstream promoter element, ChIP assays were performed in which MCF-7 and MDA-MB-231 cells were treated with formaldehyde, chromatin isolated, fragmented, and immunoprecipitated by either anti-p65 or anti-PRDX1 antibodies. Equal amounts of input DNA and immunoprecipitated DNA were quantified by real-time PCR. Each of the amplified DNA regions, named -439 and -214, includes a NF-κB binding site and are depicted in Figure 7B. Figure 7C shows a similar enrichment of the -439 and -214 sequences in the DNA immunoprecipitated by anti-p65 antibodies from MCF7 and MDA-MB-231 cell lines, demonstrating that NF-κB was bound to its two cognate sites in the *COX-2* promoter region in both cell lines. In contrast, only the chromatin immunoprecipitated from MDA-MB-231 cells by anti-PRDX1 antibodies was enriched in the -439 and -214 sequences, with the chromatin immunoprecipitated from MCF7 cells showing

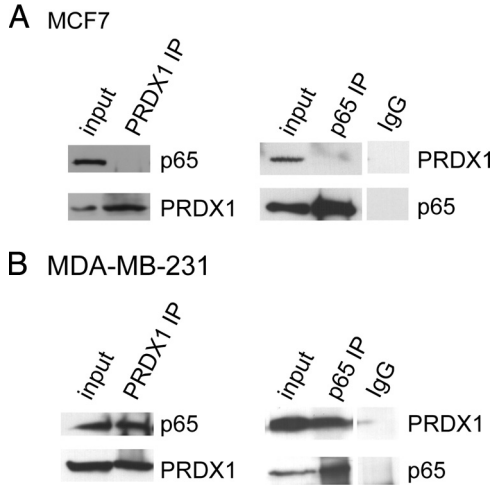

Figure 6. PRDX1 associated with NF-κB in MDA-MB-231 but not MCF7 cells. Aliquots of 500 μg of MCF7 (A) or MDA-MB-231 (B) cell lysates were incubated with anti-PRDX1, anti-NF-κB p65, or rabbit preimmune immunoglobulin G (IgG) antibodies. An input aliquot corresponding to 20 μg of total cell extracts, and the whole immunoprecipitated (IP) fractions were resolved by SDS-12% PAGE and immunoblotted with anti-NF-κB p65 or anti-PRDX1 antibodies. Data are representative of three independent experiments.

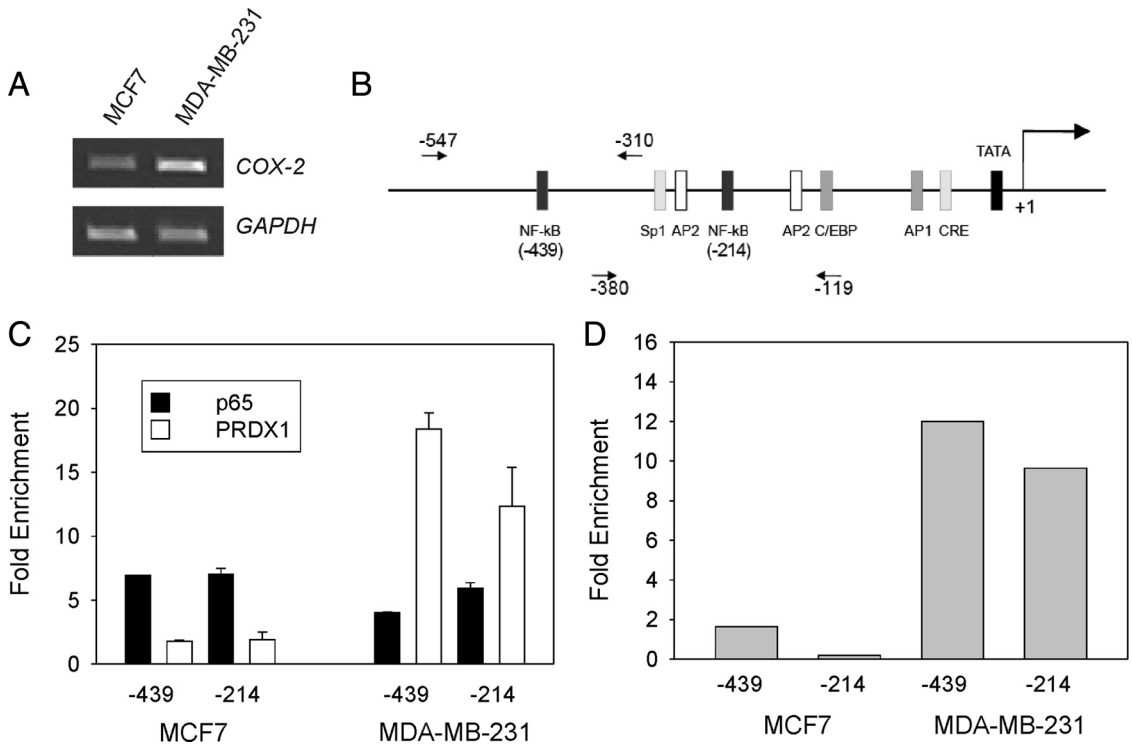

Figure 7. Increased level of *COX-2* gene expression coupled with PRDX1 and NF-κB co-occupancy of the two NF-κB recognition sites in the promoter region. (A) Total RNA was isolated from MCF7 and MDA-MB-231 cells and amplified by RT-PCR. The PCR products were resolved on a 1.5% (wt/vol) agarose gel and stained with ethidium bromide to visualize the expression levels of *COX-2* relative to *GAPDH*. Data are representative of two independent experiments. (B) Schematic representation of *COX-2* promoter showing regions amplified in the ChIP assays. (C) ChIP experiments were performed using antibodies against NF-κB p65 or PRDX1 on formaldehyde cross-linked and fragmented chromatin prepared from MCF7 and MDA-MB-231 cells. Equal amounts of input and immunoprecipitated DNA were quantified by real-time quantitative PCR for the two NF-κB binding sites. The relative enrichment in the ChIP DNA compared with the input DNA is shown. Enrichment values are the mean of three independent experiments, and the error bars represent the SE. (D) Formaldehyde cross-linked and fragmented chromatin prepared from MCF7 and MDA-MB-231 cells was subjected to immunoprecipitation first by anti-NF-κB p65 antibodies and then by anti-PRDX1 antibodies.

no enrichment in these sequences (Figure 7C). These results demonstrate that PRDX1 was associated with the *COX-2* promoter region in ER− MDA-MB-231 cells but not in ER+ MCF7 cells. To determine whether NF-κB and PRDX1 co-occupied the same *COX-2* promoter region, we performed a re-ChIP assay in which formaldehyde cross-linked and fragmented chromatin preparations from MCF7 and MDA-MB-231 cells were incubated with anti-p65 antibodies. The immunoprecipitated chromatin fraction was then subjected to a second immunoprecipitation by using anti-PRDX1 antibodies. Again, equal amounts of input DNA and immunoprecipitated DNA were quantified by real-time PCR. Figure 7D shows that the -439 and -214 sequences were not enriched in the DNA immunoprecipitated from MCF7. Conversely, DNA immunoprecipitated from MDA-MB-231 cells was enriched in both sequences, demonstrating that in ER− MDA-MB-231 cells, NF-κB and PRDX1 are associated simultaneously to the each of the NF-κB recognition sites on the *COX-2* gene.

Knockdown of PRDX1 Attenuates the Expression of COX-2 in MDA-MB-231 but Not in MCF7 Cells

To evaluate the importance of the interaction between PRDX1 and NF-κB in the expression of the *COX*-2 gene, we knocked down the levels of PRDX1 in MDA-MB-231 and MCF7 cells. We used a lentiviral vector system stably expressing shRNA to generate PRDX1 stable knockdown MDA-MB-231 and MCF7 cell lines. The transfection of an empty lentiviral vector or a vector containing a scrambled DNA sequence provided negative control cell lines. Immunoblot analysis demonstrated that the level of PRDX1 in the PRDX1 knockdown cells was reduced by 65 and 78% in clone G1-MCF7 and clone G2-MCF7 cells, respectively (Figure 8A). In the G1 and G2-MDA-MB-231 clones, PRDX1 was reduced by 77 and 73%, respectively (Figure 8B). In the G1 and G2 MDA-MB-231 clones, expression of *COX-2* was reduced to ~30% of that observed in the control-transfected cells (Figure 8D). In marked contrast, knockdown of PRDX1 expression in MCF7 cells resulted in increased expression of *COX-2* (Figure 8C).

To determine the impact of reduced expression of PRDX1 on the occupancy of NF-κB in the upstream promoter region of the *COX-2* gene in MDA-MB-231 cells, we performed ChIP assays with the control and PRDX1 knockdown MDA-MB-231 cell lines. Figure 8E shows that occupancy of p65 at the NF-κB sites (-439 and -214 regions) was reduced in the PRDX1 knockdown but not control MDA-MB-231 cell lines. Together, these observations suggest that the PRDX1 association with NF-κB has a role in the retention of NF-κB at the *COX-2* upstream promoter region in MDA-MB-231 cells.

PRDX1 Is Phosphorylated in MDA-MB-231 Cells

Because PRDX1 was expressed in both ER+ and ER− breast cancer cells, we investigated what properties of PRDX1 may

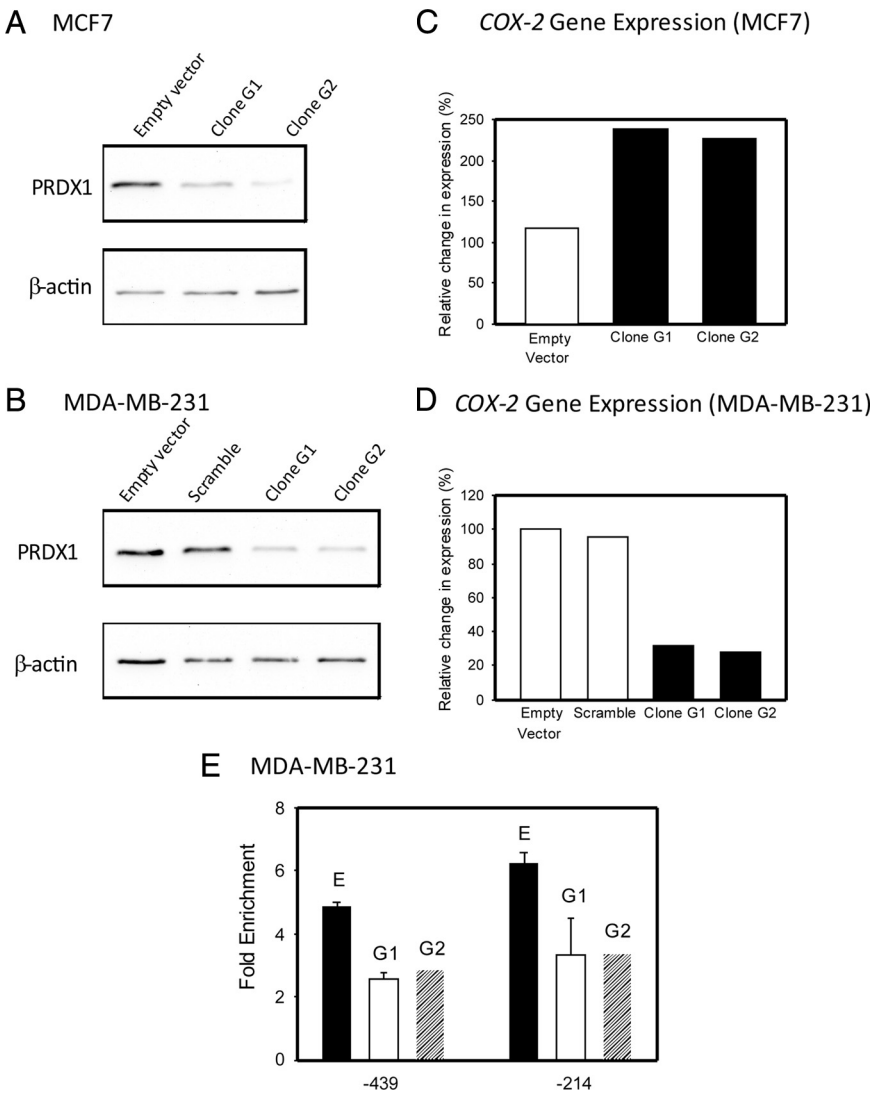

Figure 8. Knockdown of PRDX1 reduces the expression of the *COX-2* gene in MDA-MB-231 but not in MCF7 cells. Cellular proteins isolated from the control and PRDX1 knockdown (G1 and G2) MCF7 (A) and MDA-MB-231 (B) cells were resolved on SDS-12% PAGE and immunoblotted with anti-PRDX1 antibodies. Total RNA was isolated from the control and PRDX1 knockdown (G1 and G2) MCF7 (C) and MDA-MB-231 (D) cells and quantified by real-time RT-PCR. Fold change values, normalized to GAPDH levels are representative of experiments done twice. (E) ChIP assays were performed using antibodies against NF-κB p65 on formaldehyde cross-linked and fragmented chromatin prepared from control (empty vector control; E) and PRDX1 knockdown (G1 and G2) MDA-MB-231 cells as described in the legend to Figure 7.

differ in these two types of breast cancer cells that may confer the ability to associate with DNA in one cell type but not the other. To determine whether PRDX1 was differentially modified in the breast cancer cell lines, total cell extracts from MCF10A1, MCF7, and MDA-MB-231 cells were electrophoretically resolved on two-dimensional gels and analyzed by immunoblot with anti-PRDX1 antibodies. Figure 9A shows that a single PRDX1 species was detected in the MCF10A1 and MCF7 cell extracts, whereas a second more acidic species also was detected in the MDA-MB-231 cell extract. Two PRDX1 species also were detected in a preparation of proteins cross-linked to the DNA of MDA-MB-231 cells in situ by cisplatin (Figure 9B). The extract from MDA-MB-231 cells was treated with CIP before the electrophoresis to determine whether the presence of the more acidic PRDX1 species was the result of a phosphorylation event. Indeed, Figure 9C shows that the CIP treatment resulted in the disappearance of the second species, indicating that it represented a phosphorylated form of PRDX1. Moreover, Figure 9B provides evidence that phosphorylated PRDX1 was bound to DNA in MDA-MB-231 cells.

Previous reports demonstrated that oxidation of PRDX1 results in an acidic shift in two-dimensional gels. Treatment of MDA-MB-231 and MCF7 cells with H_2O_2 results in the oxidation of PRDX1, which is readily detected on immunoblots stained with an anti-PRDX1-SO_3 antibody (Supplemental Figure S1A). To determine whether oxidation is in part responsible for the acidic shift of PRDX1 isolated from MDA-MB-231 cells, two-dimensional immunoblots were stained with an anti-PRDX1-SO_3 antibody. No immunostaining with this antibody was observed (Supplemental Figure S1B).

DISCUSSION

Proteins cross-linked to DNA by cisplatin are involved in regulating the function and structure of DNA. Thus, proteins differentially cross-linked in breast cancer and normal mammary epithelial cells are likely to have roles in the cell type-specific regulation of chromatin structure and function and the biology of that cell type. In this study, we found that PRDX1 was bound to DNA in ER− cell lines, but not in ER+ human breast cancer cells and nontumorigenic mammary epithelial cell lines.

PRDX1, also known as natural killer cell enhancing factor A and proliferation-associated protein (Wood *et al*., 2003), is a multifunctional protein. It operates with thioredoxin to detoxify hydrogen peroxide, thus preventing the buildup of

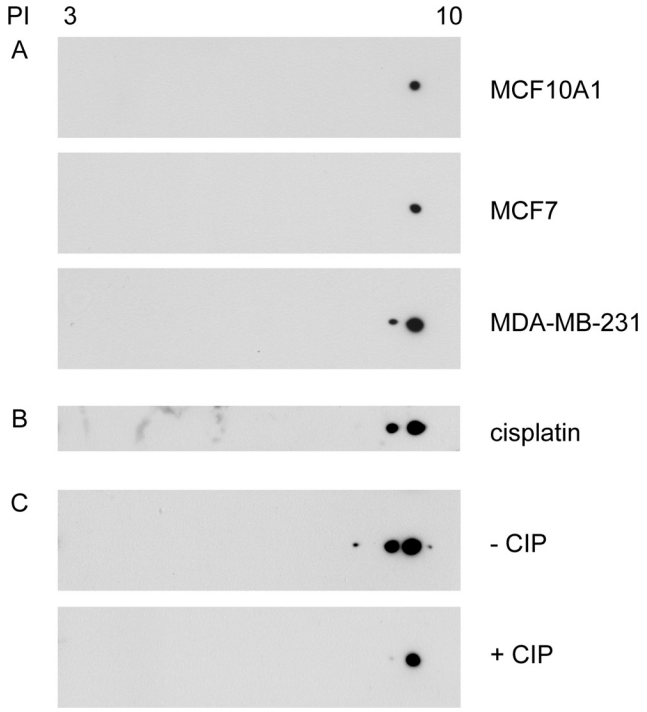

Figure 9. PRDX1 is phosphorylated in MDA-MB-231 but not MCF7 or MCF10A1 cells. Proteins (20 μg) from MCF10A1, MCF7, or MDA-MB-231 total cell lysates (A) or proteins cross-linked to DNA by cisplatin in MDA-MB-231 (B) were resolved on two-dimensional gels and immunoblotted with anti-PRDX1 antibodies. MDA-MB-231 cellular extract was treated with CIP before electrophoresis (C). Data are representative of two independent experiments.

reactive oxygen species, an accumulation of which results in oxidative stress. Alternatively, phosphorylation of PRDX1 Thr^{90} promotes the formation of a high-molecular-weight complex, and this quaternary structure change comes with a functional switch from peroxidase to chaperone activity (Jang *et al*., 2006). Moreover, although there is evidence that PRDX1 is a tumor suppressor, it also has proliferative and antiapoptotic properties (Noh *et al*., 2001; Neumann and Fang, 2007).

Although PRDX1 was more abundant in breast cancer cell lines (ER+ and ER−) than in normal or pseudonormal breast cell lines, we did not find a significant difference in PRDX1 levels between ER+ and ER− breast cancer cell lines. This result is consistent with previous data showing overexpression of PRDX1 in breast cancer tissues from most patients (87.5%) compared with normal tissues but showing no correlation between PRDX1 levels and pathological factors, including estrogen receptor status (Noh *et al*., 2001). Similarly, breast cancer cell lines had higher nuclear PRDX1 levels than a pseudonormal cell line, but there was no significant difference in nuclear PRDX1 levels between ER+ and ER− breast cancer cell lines. Nuclear PRDX1 levels were higher than cytoplasmic levels in both ER+ and ER− breast cancer cell lines, which was somewhat unexpected because PRDX1 was initially believed to be primarily located in the cytosol (Wood *et al*., 2003). However, more recent evidence revealed a PRDX1 nuclear presence (Immenschuh *et al*., 2003; Park *et al*., 2007). During the course of this study, when we performed cellular fractionations, the cellular lysis buffer was free of nonionic detergent to prevent the leaking from nuclei of PRDX1, because we had observed that PRDX1 was readily extracted from nuclei with Triton X-100.

Using indirect immunofluorescence microscopic analyses, PRDX1 was colocalized with PML nuclear bodies in ER− breast cancer cell lines. This colocalization is interesting, because PML bodies have been implicated in a variety of cellular functions, including transcriptional regulation (Bernardi and Pandolfi, 2007).

The observation that PRDX1 contributed to NF-κB transcriptional activity (Hansen *et al*., 2007) prompted us to investigate whether PRDX1 was in complex with NF-κB in ER− breast cancer cells. In addition to finding that PRDX1 was in complex with NF-κB in ER−, but not ER+ cells, we demonstrated that PRDX1 and NF-κB co-occupied NF-κB recognition sites in the *COX-2* upstream promoter region in ER− but not ER+ cells. Thus, the selective binding of PRDX1 to NF-κB in MDA-MB-231 cells provides a mechanism by which PRDX1 would be associated with nuclear DNA in MDA-MB-231 cells but not in MCF7 cells. The results of the PRDX1 knockdown studies further highlights a differential function of PRDX1 in ER− MDA-MB-231 and ER+ MCF7 cells. Previous reports have shown that increased oxidative stress results in increased *COX-2* expression (Wu *et al*., 2009). A similar response may be occurring in MCF7 cells as a consequence of knocking down PRDX1. However, in MDA-MB-231 cells knocking down PRDX1 results in decreased expression of the *COX-2* gene, consistent with a role of PRDX1 in increasing the activity, retention, or both of NF-κB on the upstream promoter region of the *COX-2* gene.

To elucidate the molecular basis of the exclusive cross-linking by cisplatin and formaldehyde of PRDX1 to the DNA of ER− cells, we analyzed PRDX1 from ER+ and ER− breast cancer cells for posttranslational modifications. A phosphorylated form of PRDX1 was present in ER−, but not ER+, breast cancer cells. This phosphorylated form was cross-linked to DNA by cisplatin. Phosphorylation of PRDX1 on Thr^{90} was shown to reduce PRDX1 peroxidase activity by 80% (Chang *et al*., 2002) and to promote oligomerization and enhance PRDX1 chaperone activity (Jang *et al*., 2006). Thus, it is possible that the chaperone activity of PRDX1 rather than its antioxidant activity plays a role in the co-occupancy of PRDX1 and NF-κB in upstream promoter elements of the *COX-2* and perhaps other NF-κB–responsive genes in ER− breast cancer cells. It was reported that, in aggressive prostate cancer cell lines, PRDX1 interacted with the androgen receptor (AR), and was bound to the androgen-responsive element (ARE) of the prostate-specific antigen (*PSA*) gene. The stimulation of AR transactivation by PRDX1 was independent of the PRDX1 peroxidase activity (Park *et al*., 2007). However, this binding of PRDX1 to the *PSA* gene ARE only occurred under hypoxia/reoxygenation, a cell culture condition mimicking the variable oxygenation typical of tumor tissues (Park *et al*., 2007). In contrast, PRDX1 and NF-κB were loaded simultaneously onto the *COX-2* upstream promoter element in normally cycling MDA MB 231 ER− breast cancer cells.

NF-κB, as a critical transcription factor regulating the expression of a plethora of genes, interacts with a number of regulators controlling its activity, including several chaperones (Mankan *et al*., 2009). Deregulation of NF-κB activity has been implicated in the development of various inflammatory and autoimmune diseases, as well as in the development of tumors. This study has identified PRDX1 as a protein that interacts with NF-κB at the DNA level and presumably modulates its transcriptional activity in ER− breast cancer cells. As such, PRDX1 is a potential target in the treatment of endocrine-nonresponsive breast tumors.

ACKNOWLEDGMENTS

We thank Dr. Sam Kam-Pun Kung for help with the production of the lentiviral vectors. This research was supported by grants from CancerCare Manitoba Foundation, Canadian Breast Cancer Foundation, and a Canada Research Chair (to J.R.D.).

REFERENCES

Allred, D. C., O'Connell, P., and Fuqua, S.A.W. (1993). Biomarkers in early breast neoplasia. J. Cell. Biochem. *17G*, 125–131.

Batty, E., Jensen, K., and Freemont, P. (2009). PML nuclear bodies and their spatial relationships in the mammalian cell nucleus. Front. Biosci. *14*, 1182–1196.

Bernardi, R., and Pandolfi, P. P. (2007). Structure, dynamics and functions of promyelocytic leukaemia nuclear bodies. Nat. Rev. Mol. Cell Biol. *8*, 1006–1016.

Chang, T. S., Jeong, W., Choi, S. Y., Yu, S., Kang, S. W., and Rhee, S. G. (2002). Regulation of peroxiredoxin I activity by Cdc2-mediated phosphorylation. J. Biol. Chem. *277*, 25370–25376.

Chichiarelli, S., Coppari, S., Turano, C., Eufemi, M., Altieri, F., and Ferraro, A. (2002). Immunoprecipitation of DNA-protein complexes cross-linked by cis-diamminedichloroplatinum. Anal. Biochem. *302*, 224–229.

Coutts, A. S., Leygue, E., and Murphy, L. C. (1999). Variant estrogen receptor-alpha messenger RNA expression in hormone-independent human breast cancer cells. J. Mol. Endocrinol. *23*, 325–336.

Davie, J. R., Samuel, S. K., Spencer, V. A., Holth, L. T., Chadee, D. N., Peltier, C. P., Sun, J.-M., Chen, H. Y., and Wright, J. A. (1999). Organization of chromatin in cancer cells: role of signalling pathways. Biochem. Cell Biol. *77*, 265–275.

Drobic, B., Perez-Cadahia, B., and Davie, J. R. (2010). Promoter chromatin remodeling of immediate-early genes is mediated through H3 phosphoryalation at either serine 28 or serine 10 by the MSK1 multi-protein complex. Nucleic Acids Res. *38*, 3196–3208.

Ferraro, A., Grandi, P., Eufemi, M., Altieri, F., and Turano, C. (1992). Crosslinking of nuclear proteins to DNA by cis-diamminedichloroplatinum in intact cells. Involvement of nuclear matrix proteins. FEBS Lett. *307*, 383–385.

Hansen, J. M., Moriarty-Craige, S., and Jones, D. P. (2007). Nuclear and cytoplasmic peroxiredoxin-1 differentially regulate NF-kappaB activities. Free Radic. Biol. Med. *43*, 282–288.

He, S., Sun, J. M., Li, L., and Davie, J. R. (2005). Differential intranuclear organization of transcription factors Sp1 and Sp3. Mol. Biol. Cell *16*, 4073–4083.

Immenschuh, S., Baumgart-Vogt, E., Tan, M., Iwahara, S., Ramadori, G., and Fahimi, H. D. (2003). Differential cellular and subcellular localization of heme-binding protein 23/peroxiredoxin I and heme oxygenase-1 in rat liver. J. Histochem. Cytochem. *51*, 1621–1631.

Ishov, A. M., Stenberg, R. M., and Maul, G. G. (1997). Human cytomegalovirus immediate early interaction with host nuclear structures: definition of an immediate transcript environment. J. Cell Biol. *138*, 5–16.

Jang, H. H., *et al*. (2006). Phosphorylation and concomitant structural changes in human 2-Cys peroxiredoxin isotype I differentially regulate its peroxidase and molecular chaperone functions. FEBS Lett. *580*, 351–355.

Li, L., and Davie, J. R. (2008). Association of Sp3 and estrogen receptor alpha with the transcriptionally active trefoil factor 1 promoter in MCF-7 breast cancer cells. J. Cell. Biochem. *105*, 365–369.

Mankan, A. K., Lawless, M. W., Gray, S. G., Kelleher, D., and McManus, R. (2009). NF-kappaB regulation: the nuclear response. J. Cell Mol. Med. *13*, 631–643.

Meng, X., and Wilkins, J. A. (2005). Compositional characterization of the cytoskeleton of NK-like cells. J. Proteome. Res. *4*, 2081–2087.

Neumann, C. A., and Fang, Q. (2007). Are peroxiredoxins tumor suppressors? Curr. Opin. Pharmacol. *7*, 375–380.

Neve, R. M., *et al*. (2006). A collection of breast cancer cell lines for the study of functionally distinct cancer subtypes. Cancer Cell *10*, 515–527.

Noh, D. Y., Ahn, S. J., Lee, R. A., Kim, S. W., Park, I. A., and Chae, H. Z. (2001). Overexpression of peroxiredoxin in human breast cancer. Anticancer Res. *21*, 2085–2090.

Park, S. Y., Yu, X., Ip, C., Mohler, J. L., Bogner, P. N., and Park, Y. M. (2007). Peroxiredoxin 1 interacts with androgen receptor and enhances its transactivation. Cancer Res. *67*, 9294–9303.

Samuel, S. K., Minish, M. M., and Davie, J. R. (1997). Nuclear matrix proteins in well and poorly differentiated human breast cancer cell lines. J. Cell. Biochem. *66*, 9–15.

Samuel, S. K., Spencer, V. A., Bajno, L., Sun, J.-M., Holth, L. T., Oesterreich, S., and Davie, J. R. (1998). In situ cross-linking by cisplatin of nuclear matrix-bound transcription factors to nuclear DNA of human breast cancer cells. Cancer Res. *58*, 3004–3008.

Singh-Ranger, G., Salhab, M., and Mokbel, K. (2008). The role of cyclooxygenase-2 in breast cancer: review. Breast Cancer Res. Treat. *109*, 189–198.

Spector, D. L. (2006). SnapShot: cellular bodies. Cell *127*, 1071

Spencer, V. A., and Davie, J. R. (2002a). Isolation of proteins cross-linked to DNA by cisplatin. In: The Protein Protocols Handbook, ed. J. M. Walker, Totowa, NJ: Humana Press, 747–752.

Spencer, V. A., and Davie, J .R. (2002b). Isolation of proteins cross-linked to DNA by formaldehyde. In: The Protein Protocols Handbook, ed. J. M. Walker, Totowa, NJ: Humana Press, 753–760.

Spencer, V. A., Samuel, S. K., and Davie, J. R. (2000). Nuclear matrix proteins associated with DNA *in situ* in hormone-dependent and hormone-independent human breast cancer cell lines. Cancer Res. *60*, 288–292.

Spencer, V. A., Samuel, S. K., and Davie, J. R. (2001). Altered profiles in nuclear matrix proteins associated with DNA in situ during progression of breast cancer cells. Cancer Res. *61*, 1362–1366.

Sun, J. M., Chen, H. Y., and Davie, J. R. (2007). Differential distribution of unmodified and phosphorylated histone deacetylase 2 in chromatin. J. Biol. Chem. *282*, 33227–33236.

Sun, J. M., Chen, H. Y., Moniwa, M., Litchfield, D. W., Seto, E., and Davie, J. R. (2002). The transcriptional repressor Sp3 is associated with CK2 phosphorylated histone deacetylase 2. J. Biol. Chem. *277*, 35783–35786.

Sun, J.-M., Chen, H. Y., and Davie, J. R. (2001). Effect of estradiol on histone acetylation dynamics in human breast cancer cells. J. Biol. Chem. *276*, 49435–49442.

Vargo-Gogola, T., and Rosen, J. M. (2007). Modelling breast cancer: one size does not fit all. Nat. Rev. Cancer *7*, 659–672.

Wood, Z. A., Schroder, E., Robin, H. J., and Poole, L. B. (2003). Structure, mechanism and regulation of peroxiredoxins. Trends Biochem. Sci. *28*, 32–40.

Wu, N., Siow, Y. L., and O, K. (2009). Induction of hepatic cyclooxygenase-2 by hyperhomocysteinemia via nuclear factor-kappaB activation. Am. J. Physiol. Regul. Integr. Comp. Physiol. *297*, R1086–R1094.

Zhu, Y., Wang, A., Liu, M. C., Zwart, A., Lee, R. Y., Gallagher, A., Wang, Y., Miller, W. R., Dixon, J. M., and Clarke, R. (2006). Estrogen receptor alpha positive breast tumors and breast cancer cell lines share similarities in their transcriptome data structures. Int. J. Oncol. *29*, 1581–1589.